

Atomic configurations of Pd atoms in PdAu(111) bimetallic surfaces investigated using the first-principles pseudopotential plane wave approach

Dingwang Yuan,^{1,2} Xingao Gong,³ and Ruqian Wu¹

¹*Department of Physics and Astronomy, University of California, Irvine, California 92697-4575, USA*

²*ICTS, Chinese Academy of Sciences, Beijing, 100080, China*

³*Surface Science Laboratory and Department of Physics, Fudan University, Shanghai-200433, China*

(Received 22 November 2006; revised manuscript received 5 February 2007; published 16 February 2007)

Atomic configurations of two or three Pd substituents on the Au(111) surface are investigated using the first-principles pseudopotential plane wave approach. Pd atoms are found to form second neighborhoods on PdAu(111). The Pd-*d* band becomes narrow and well below the Fermi level, very different from those in a Pd film or bulk Pd. Yet the surface Pd atoms are still active and serve as independent attractive centers towards adsorbates. The special ensembles are important for catalysis applications because of their ability to confine reactants in a small region.

DOI: [10.1103/PhysRevB.75.085428](https://doi.org/10.1103/PhysRevB.75.085428)

PACS number(s): 68.35.Dv, 68.43.Bc, 71.15.Mb, 71.20.Gj

I. INTRODUCTION

In order to design and fabricate excellent bimetallic structures for catalysis applications, it is crucial to find efficient ways to control their chemical properties by manipulating lattice strain, constituents, and growth conditions.¹⁻⁹ In general, catalytic reactivity of bimetallic surface depends on the ligand effects associated with charge transfer, orbital rehybridization, and lattice strain.^{3,4,10,11} However, it has been recently recognized that the ensemble effect, associated with particular distribution patterns of active constituents, may play a key role in promoting chemical reactions.^{2,6} The unusually high reactivity and selectivity of the PdAu(001) bimetallic catalyst towards vinyl acetate (VA) synthesis, for instance, mainly stems from the presence of second neighbor Pd pairs on Au(001)^{12,13} that provide appropriate distance between reactants. Unlike the ligand effects, however, it is technically difficult to characterize the ensemble effects through experimental approaches; thereby systematic theoretical studies are highly desired.

Although the presence of different ensembles can be inspected using the scanning tunneling microscope (STM), very few atomic resolution images have been reported.⁶ More often, the existence of different ensembles are probed with ethylene, CO, and H, using various surface sensitive techniques such as infrared reflection absorption spectroscopy (IRAS) and temperature programmed desorption (TPD).^{7,8} For PdAu bimetallic surfaces, which are among the most important mixed-metal catalysts, it is well established that Au tends to segregate to the surface even at moderate temperatures¹⁴ because of the difference in their surface energies. The morphology of PdAu surfaces strongly depends on the experimental condition and annealing history.¹⁵⁻¹⁷ Several compositions on the PdAu bimetallic surfaces were reported, including the ordered surface alloy phase,^{16,17} the Pd overlayer on Au(111),^{14,15} and random Pd-Au(111) alloy surfaces with varying Pd ensembles.⁶⁻⁸ For instance, from STM images and infrared data, Behm *et al.* concluded that the critical ensemble for CO adsorption on PdAu(111) is Pd monomer.⁶ This conclusion was supported by the extensive work of Goodman's group,⁸ they found only one feature at

2087 cm⁻¹ in IRAS for CO/PdAu(111) if the substrate is annealed up to 800 K. However, the correlation between experimental features and surface configurations have not yet been clearly established, and theoretical studies are therefore required to attain comprehensive understandings. Furthermore, ensembles with second neighbor Pd are seldom separated from isolated monomers. Since reactants confined in a region smaller than 5 Å should have enormous opportunity to interact, the former may play a significant role in catalysis applications and deserves special attention.

In this paper, we report results of energetic and electronic properties of the PdAu(111) bimetallic surfaces using state-of-the-art density functional approaches. The formation of second neighbor Pd ensembles is found to be more energetically favorable, especially around subsurface Pd dopants. This stems from the fact that the Pd-Au bond is stronger than the Pd-Pd and Au-Au bonds. Moreover, each Pd in these ensembles behaves like an independent attractive center on the PdAu bimetallic surfaces towards small foreign molecules such as CO. The theoretical results for adsorption energies and CO stretch frequencies agree well with experimental data. After description for the computational details in Sec. II, we discuss results of the formation of Pd ensembles and their features towards CO adsorbates in Sec. III. A brief summary will be given in Sec. IV.

II. COMPUTATIONAL DETAILS

The calculations are performed in the framework of density functional theory (DFT), using the generalized gradient approximation (GGA) for the description of exchange-correlation interaction.¹⁸ The effects of ionic cores are represented by ultrasoft pseudopotentials,¹⁹ as implemented in the Vienna *ab initio* Simulation Package (VASP).²⁰ The Au(111) surface is modeled with a 5-layer Au slab and a 15 Å vacuum in between. In the lateral plane, we use a 4×4 supercell so as to mimic cases with lower Pd concentration and sparse CO adsorption. Plane waves with an energy cutoff of 350 eV are used to expand wave functions, while integrals in the reciprocal space are evaluated through summations over 5×5×1 *k* points in the Monkhorst-Pack grids.²¹ The self-

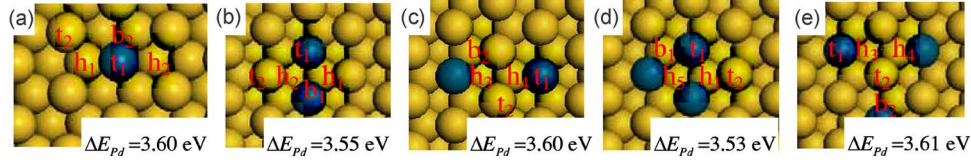


FIG. 1. (Color online) The calculated formation energies of selected ensembles with two and three Pd dopants (in blue or dark) in the surface layer of PdAu(111).

consistence is assumed when the total energy difference between two adjacent steps becomes smaller than 10^{-4} eV. The two bottommost Au layers are frozen at their bulk positions, whereas all the other atoms are fully relaxed with a criterion that requires having the calculated atomic forces smaller than 0.03 eV/Å on each ion. As known, GGA calculations overestimate the lattice sizes of Au and Pd by 2%. To circumvent the “artificial stresses” in structural optimization procedures, we use the theoretical lattice size for the bulk Au, $a_{Au} = 4.18$ Å, in the lateral plane throughout the calculations. Although most calculations were performed with the nonspin polarized GGA scheme, we conducted test calculations for selected systems with spin polarization (i.e., GGSA). As expected, they converged to the nonmagnetic ground states, as produced by regular GGA calculations.

We considered substitutions of one, two, or three Pd atoms in the topmost and subsurface layers of the Au(111) surface. In order to characterize the thermal stability of different Pd configurations, especially those with different numbers of Pd atoms, we define the formation energy for cases in Fig. 1 as

$$\Delta E_{Pd} = -[E_{PdAu} - E_{Au-slab} + N_{Pd}(E_{Au-bulk} - E_{Pd-atom})]/N_{Pd}. \quad (1)$$

Here, E_{PdAu} , $E_{Au-surf}$, $E_{Au-bulk}$, and $E_{Pd-atom}$ represent the total energies of the PdAu surface, clean Au(111) slab, bulk gold (per atom),²² and isolated Pd atom, respectively. N_{Pd} is the number of Pd atoms in the unit cell. This definition is well accepted in the literature for the studies of alloy formation, impurity segregation and chemisorption. Of course, one can use $E_{Pd-bulk}$ instead of $E_{Pd-atom}$ in Eq. (1) if the reservoirs of both Au and Pd are assumed to be bulklike. Nevertheless, this only causes a parallel shift in ΔE_{Pd} and will not affect discussions in the next section.

When one Pd atom is placed in the subsurface layer, as shown in Fig. 2, the formation energy for each Pd in the surface layer is defined as

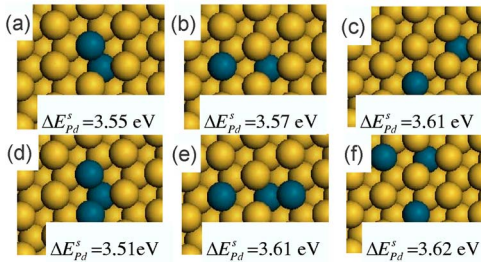


FIG. 2. (Color online) Calculated formation energies of selected ensembles with one Pd atom in the subsurface layer of PdAu(111).

$$\Delta E_{Pd}^s = -[E_{PdAu} - E_{Au+Pd(sub)} + N_{Pd}^s(E_{Au-bulk} - E_{Pd-atom})]/N_{Pd}^s, \quad (2)$$

where $E_{Au+Pd(sub)}$ is the total energy of Au slab with one Pd atom embedded in the subsurface layer, and N_{Pd}^s is the number of Pd atoms in the surface layer only. This is a necessary step for meaningful comparison between different surface ensembles, since Pd in the interior region is lower in formation energy by as much as 0.35 eV per atom.

Finally, we probed the surface activity of the PdAu bimetallic surfaces with a CO molecule. The adsorption energy of CO is defined as

$$E_{ad} = -(E_{CO/PdAu} - E_{PdAu} - E_{CO}), \quad (3)$$

where $E_{CO/PdAu}$ is the total energy of CO-adsorbed PdAu surface, E_{CO} is the total energy of a CO molecule in its gas phase, and E_{PdAu} is the total energy of the PdAu bimetallic surface.

III. RESULTS AND DISCUSSIONS

A. Pd monomer formation on Au(111) surface

To quantitatively represent the energetic and thermal stability of different Pd ensembles, we can use the formation energies from Eq. (1) and the differences in total energies. The data of ΔE_{Pd} for different ensembles on the PdAu(111) surface are presented in Fig. 1. It is obvious that ensembles consisting of first neighbor Pd pairs [e.g., 1(b) and 1(d)] are energetically unfavorable. For instance, ensembles 1(b) and 1(c) have the same set of atoms but the former is higher in total energy by 0.10 eV (or 0.05 eV in ΔE_{Pd}). The total energy difference between the other two comparable ensembles, 1(d) and 1(e), is even larger by 0.26 eV. According to a rough estimation based on the standard Boltzmann distribution model, the population ratio between 1(b) and 1(c) is smaller than 5% at room temperature while the chances of having ensemble 1(d) is negligible. Although such population analyzes are rather qualitative since experimental samples are not in their thermal equilibrium, our results reasonably explain the observation made by Maroun *et al.*⁶ from the atomic scale STM images, where Pd atoms predominantly form “monomers.”

The absence of nearest Pd neighborhoods can be explained through an approximate pair-interaction model. By using total energies of the bulk Au, bulk Pd, and bulk PdAu alloy, we find that the energies associated with each Au-Au, Pd-Pd, and Pd-Au bond are 0.249 eV, 0.307 eV, and 0.317 eV, respectively. Accordingly, ΔE_{Pd} defined in Eq. (1) for configurations in Fig. 1 can be estimated in eV through the pair-interaction model as

$$\Delta E_{\text{Pd}} = (0.058 * N_{\text{Pd-Pd}} + 0.068 * N_{\text{Pd-Au}}) / N_{\text{Pd}} + 2.992, \quad (4)$$

where $N_{\text{Pd-Pd}}$ and $N_{\text{Pd-Au}}$ are numbers of Pd-Pd and Pd-Au bonds, and 2.992 eV denotes the formation energy of each bulk Au. Surprisingly, Eq. (4) produces well the formation energies of different Pd ensembles in Fig. 1, i.e., 3.56 eV for ensemble 1(b) and 3.52 eV for ensemble 1(d). This indicates that the disturbance of Pd substituents is limited within a short range, not much beyond their first neighborhoods. The high strength of Pd-Au bonds is obviously the key factor that promotes segregation of surface Pd atoms toward subsurface or interior layers, and prevents the formation of Pd first neighborhoods. This same reason was used to explain the distribution of Pd on PdCu surfaces deposited on Ru(0001) (Ref. 23) as well as in ordered and disordered of bulk alloys.²⁴

Significantly, we find that it is energetically more stable for Pd atoms to form various second neighbor ensembles. For example, ensemble 1(e) is 0.03 eV higher in total energy than three isolated monomers and the population ratio between 1(e) and 1(a) should be close to one-to-one at room temperature. As a matter of fact, the distribution of Pd in the atomic scale STM images for PdAu(111) (Ref. 6) is disordered and ensembles 1(c) and 1(e) can be found in several places. On PdAu(001), ΔE_{Pd} of ensembles comprising two (3.61 eV) or three (3.63 eV) Pd second neighborhoods are remarkably larger than that of an isolated Pd monomer (3.57 eV). Therefore, the population ratio between Pd second neighborhoods and individual monomers should be even higher there. Since the second neighbor distances on Au(111) and Au(001) are only 4.99 Å and 4.08 Å, not much larger than sizes of many reactants, it is essential to discuss second neighbor ensembles separately from isolated Pd monomers. Particularly, second neighbor ensembles may confine several reactants in a small range for their consequent reaction.¹³

Since most Pd atoms segregate into the interior region, it is important to investigate their influence on the formation of surface ensembles, particularly from the subsurface substituents. Using the formation energy of each surface atom defined in Eq. (2), we present Pd formation energies including the subsurface effects in Fig. 2. Again, neither surface-surface nor surface-subsurface first Pd neighbors are energetically favorable. Figure 2(f) is more stable than 2(d) [or 2(e)] with 0.21 eV (or 0.02 eV). However, the total energy difference is only 0.10 eV between 1(b) and 1(c). Then, the presence of subsurface Pd further promotes the formation of second neighbor Pd dimers in the topmost layer, which also manifested by values of $\Delta E_{\text{Pd}}^{\text{s}}$ for ensembles 2(e) 2(f).

To understand why the Pd-Au bond is so strong and also to access the chemical properties of PdAu(111), the projected density of d-states (PDOS) are plotted in Fig. 3 for the Pd atom and the adjacent Au in ensembles 1(a) 1(c). While the PDOS of Au-*d* band remains almost unaffected from that of the clean Au(111) surface, the Pd-*d* band becomes very narrow and the main peak lies well below the Fermi level. From the charge density difference shown in the inset, it is clear that the effect of a Pd substituent is limited to its first neighbors. Pd experiences weak hybridization with surrounding

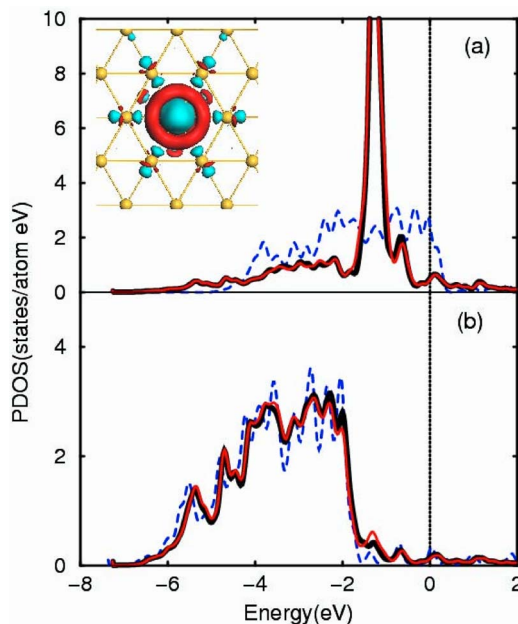


FIG. 3. (Color online) The projected density of d-states of Pd (in panel a) and adjacent Au (in panel b) in the PdAu(111) surface with ensembles displayed in Fig. 1(a) (bold black lines) and 1(c) (red/thin lines). Dashed lines are PDOS of the clean Au(111) and Pd(111) surfaces. Inset shows the top view of charge difference $\Delta\rho = \rho_{\text{PdAu}} - \rho_{\text{Au}} - \rho_{\text{Pd,atom}}$. The red (dark) and cyan (light) regions represent charge accumulation and depletion, respectively.

Au atoms and its atomistic properties are somewhat restored. The vanishing Pd-*d* holes and ring shape [shell shape in three-dimensional (3D)] of charge accumulation in Fig. 3(a) suggest onsite *s-d* charge transfer along with a small amount of Au-to-Pd charge transfer. Since Pd-Au bond encompasses visible ionic features, the Pd-Au formation energy is large despite their weak hybridization.

B. CO adsorption on PdAu(111) surface

From the PDOS alone, one may perceive that Pd should not be much more active than Cu towards adsorbates. Meanwhile, Au sites are still inactive because of the negligible change in Au-PDOS from Au(111) to PdAu(111). To examine the local chemical properties, it is useful to calculate the chemisorption energy and site preference of various small molecules such as CO. In Table I, we present the calculated adsorption energy (E_{ad}) defined by Eq. (4) and stretching frequencies (f) of CO on different ensembles of PdAu(111). As known, DFT-GGA calculations usually overestimate the adsorption energies (E_{ad}) of CO because of the incorrect description for the CO- $2\pi^*$ orbital.²⁵ The revised Perdew-Burke-Ernzerhof (RPBE) functional, extrapolation method, and GGA+U type functional offer some improvement.²⁶⁻²⁸ For instance, the PW91 functional gives small but meaningful E_{ad} for weak CO adsorption on Au(111), in poor accordance with experimental observations. In contrast, the RPBE functional appropriately reduces E_{ad} to almost zero as shown in Table I. Meanwhile, RPBE also improves the agreement in E_{ad} for CO adsorbed on Pd(111) between theory and experi-

TABLE I. The GGA-PW91 results of adsorption energies, E_{ad} (in eV), and stretching frequency, f (in cm^{-1}) of CO adsorbate on different surfaces. The abbreviations of adsorption sites are marked in Fig. 1 for different ensembles. Results in brackets are produced with the RPBE functionals.

System	Site	E_{ad} (eV)	F (cm^{-1})
Pd(111)	atop	1.39[1.15]	2040
	fcc-hollow	2.06[1.80]	1766
	hcp-hollow	2.04[1.76]	1770
	bridge	1.85[1.57]	1854
Au(111)	atop	0.22[-0.04]	2048
	fcc-hollow	0.20[-0.04]	1819
	hcp-hollow	0.21[-0.07]	1838
PdAu(111)-1a	t_1	1.11	2056
	t_2	0.28	2068
	h_1	0.78	1854
	h_2	0.79	1815
	b_2	0.82	1895
PdAu(111)-1b	t_1	1.23	2046
	t_2	0.32	2069
	h_1	1.41	1809
	h_2	1.43	1800
	b_1	1.54	1861
PdAu(111)-1c	t_1	1.17	2043
	t_2	0.30	2045
	h_3	0.91	1806
	h_4	0.88	1800
	b_2	0.96	1907
PdAu(111)-1d	t_1	1.25	2050
	t_2	0.35	2067
	h_1	1.46	1807
	h_5	1.93	1774
	b_1	1.67	1868
PdAu(111)-1e	t_1	1.16	2049
	t_2	0.31	2070
	h_3	0.92	1781
	h_4	0.90	1824
	b_2	0.94	1889

ment, 1.80 eV vs 1.47–1.53 eV.²⁹ Nevertheless, PW91 and RPBE functionals produce the same preferential sites and the RPBE correction to E_{ad} is predictable, 0.2–0.3 eV. Calculations with the PW91 functional alone should be sufficient for studies of the ensemble effect for CO/PdAu(111).

On the preferential ensembles 1(a) 1(c) 1(e) of PdAu(111), CO strongly prefers the t_1 (on Pd, cf. the site notations in Fig. 1) site. Since 1(a) 1(c) 1(e) are major ensembles on PdAu(111), one should observe that CO binds primarily to the top sites. This agrees well with the results found by Behm's and Goodman's groups.^{6,7} The calculated CO stretching frequencies on ensemble 1(a) 1(c) 1(e) are

2043–2056 cm^{-1} , as compared to experimental value of 2087 cm^{-1} (the deviation of 40 cm^{-1} is caused by GGA). Evidently, it is quite difficult to distinguish these three ensembles through TPS and IRAS measurements with CO adsorption since they share almost identical values of either E_{ad} or f . To this end, larger molecules might be used to probe the second neighbor ensembles, but the explanation of experimental data is expected to be more intricate. For instance, our separate calculations indicate that the addition of a second neighbor Pd increases the adsorption energy of ethylene on PdAu(001) from 0.56 eV to 0.69 eV.

It is worth mentioning that CO takes the threefold hollow site only on the least favorable Pd₃ ensemble [i.e., 1(d)], where the adsorption energy is large 1.93 eV. On the Pd₂Au ensemble [i.e. 1(b)], CO prefers the bridge site between Pd atoms and E_{ad} is 1.54 eV. As a result, the CO stretch frequencies (1774 cm^{-1} and 1861 cm^{-1} , respectively) are significantly reduced in these geometries since CO bond strength is much weakened through hybridization with Pd atoms underneath. Experimentally, two features are observed in the IRAS, 2087 cm^{-1} and 1940 cm^{-1} , for CO adsorbed on a 5 ML Pd/5 ML Au surface if the surface is annealed to 600 K only. The second feature is close to the calculated frequency for CO on the ensemble 1(b), 1861 cm^{-1} . However, this feature disappears if the surface is annealed up to 800 K, which can be attributed to the removal of first Pd neighborhoods.

On bimetallic surfaces, E_{ad} for adsorbates should be influenced by both ligand and ensemble effects. For CO on PdAu(111), the ligand effects are manifested by the d -band narrowing and charge redistribution in Fig. 3, and also by the fact that E_{ad} is reduced to 1.11–1.25 eV over the t_1 site on PdAu(111) from 1.39 eV over the atop site on Pd(111). Nevertheless, due to the strong screening effect of Au lattice, the ligand effects remain almost unchanged in different configurations. The modification in adsorption energy and site preference of CO on the PdAu(111) bimetallic surfaces is mainly governed by the ensemble effects. As far as from the magnitude of E_{ad} , the PdAu bimetallic surfaces are likewise active as the Pd surface. Moreover, each Pd surrounded by Au serves as a strong attractive center towards adsorbates, a benign factor that facilitates chemical reactions over Pd second neighborhoods.

Finally, we want explore the mechanism of CO-PdAu(111) interaction. From the PDOS curves for CO/PdAu(111) in Fig. 4, one can see that Pd- d states above -1 eV are hardly disturbed by CO. This excludes the possibility of having major charge transfer between CO and PdAu(111). The main change in the CO side is the remarkable broadening of the $2\pi^*$ peak. Meanwhile, noticeable shifts are found for Pd states, from the main peak at -1.6 eV to the low energy regime. The resonant features suggest that the CO and Pd interact chiefly through hybridization between the CO- $2\pi^*$ orbital and Pd- d states. From the charge density difference displayed in the inset, one can find that electrons deplete from CO- 5σ and Pd- d_{z^2} states but fill the CO- $2\pi^*$ and Pd- d_{xy} states. Apart from the exceptional charge accumulation (red region) right above Pd, the renowned mechanism of CO-metal interaction, namely via donation from the CO- 5σ state to metal and back donation from metal

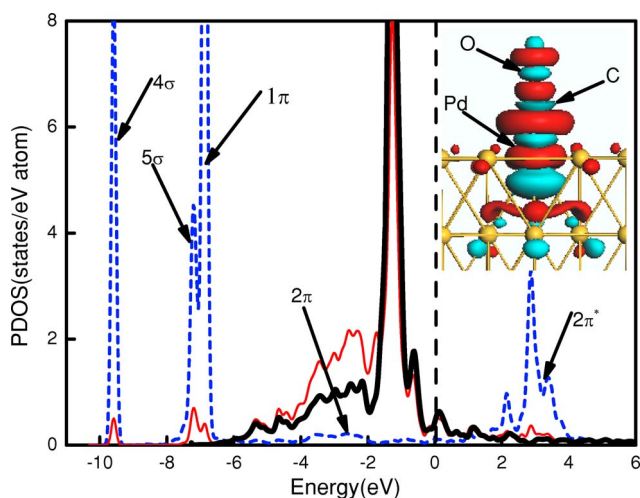


FIG. 4. (Color online) The PDOS of CO (dashed lines) and Pd/red/(thin lines) in CO/PdAu(111) on the t_1 site, accompanied by the PDOS of Pd (bold line) in the clean PdAu(111) surface. The inset displays the charge redistribution $\Delta\rho = \rho_{\text{CO/Pd+Au}} - \rho_{\text{CO}} + \rho_{\text{Pd+Au}}$. The red/dark and cyan/light regions represent charge accumulation and depletion, respectively.

to the $\text{CO-}2\pi^*$ state,¹¹ seems still applicable for CO/PdAu(111). The high activity of Pd in PdAu(111) results from the fact that Pd is ionic and has more electrons to share with adsorbates.

IV. CONCLUSION

Using the first principles pseudopotential plane wave method, we studied the energetic stability of various en-

sembles on the PdAu(111) bimetallic surface. Our results explained the absence of nearest Pd neighborhoods and, significantly, reveal the existence of second neighbor ensembles. The Pd-Au bond is found to be slightly ionic, and is stronger than Au-Au and even Pd-Pd bonds. The disturbance of Pd substituent is effectively screened by the Au lattice, not much beyond its first neighborhoods. Significantly, the adsorption energy of PdAu(111) towards CO is still comparable to that of pure Pd(111) on the top of Pd atom. Therefore, Pd atoms are strong attractive centers for foreign adsorbates, and the second neighbor ensembles may trap several reactants in a small region, which is necessary for imminent chemical reactions. The ensemble effects thereby should be carefully addressed in the future research in this direction, which may eventually bring about efficient approaches towards the rational search and design of bimetallic nanocatalysts.

ACKNOWLEDGMENTS

R.W. acknowledges helpful suggestions of D. W. Goodman. Work was supported by the DOE-BES (Grant No: DE-FG02-04ER15611). D.Y. was also supported by the ICTS, Chinese Academy of Science. X.G. was supported by the NSF of China, the national program for the basic research and research program of Shanghai. Calculations are performed on supercomputers in the NERSC.

- ¹J. H. Sinfelt, *Bimetallic Catalysis: Discoveries, Concepts and Applications* (Wiley, New York, 1983).
- ²J. A. Rodriguez, *Surf. Sci. Rep.* **24**, 223 (1996).
- ³M. Mavrikakis, B. Hammer, and J. K. Nørskov, *Phys. Rev. Lett.* **81**, 2819 (1998).
- ⁴R. Kitchin, J. K. Nørskov, M. A. Barteau, and J. G. Chen, *Phys. Rev. Lett.* **93**, 156801 (2004).
- ⁵Y. Gauthier, M. Schmid, S. Padovani, E. Lundgren, V. Bus, G. Kresse, J. Redinger, and P. Varga, *Phys. Rev. Lett.* **87**, 036103 (2001).
- ⁶F. Maroun, F. Ozanam, O. M. Magnussen, and R. J. Behm, *Science* **293**, 1811 (2001).
- ⁷C. W. Yi, K. Luo, T. Wei, and D. W. Goodman, *J. Phys. Chem. B* **109**, 18535 (2005).
- ⁸K. Luo, T. Wei, C. W. Yi, S. Axnanda, and D. W. Goodman, *J. Phys. Chem. B* **109**, 23517 (2005).
- ⁹A. Groß, *Top. Catal.* **37**, 29 (2006).
- ¹⁰J. A. Rodriguez and D. W. Goodman, *Science* **257**, 897 (1992).
- ¹¹B. Hammer, Y. Morikawa, and J. K. Nørskov, *Phys. Rev. Lett.* **76**, 2141 (1996).
- ¹²Y. F. Han, J. H. Wang, D. Kumar, Z. Yan, and D. W. Goodman, *J. Catal.* **232**, 467 (2005).
- ¹³M. S. Chen, D. Kumar, C. W. Yi, and D. W. Goodman, *Science* **310**, 291 (2005).
- ¹⁴B. E. Koel, A. Sellidj, and M. T. Paffett, *Phys. Rev. B* **46**, 7846 (1992); A. Sellidj and B. E. Koel, *ibid.* **49**, 8367 (1994).
- ¹⁵X. Y. Shen, D. J. Frankel, J. C. Hermanson, G. J. Lapeyre, and R. J. Smith, *Phys. Rev. B* **32**, 2120 (1985); **33**, 5372 (1986).
- ¹⁶C. J. Baddeley, C. J. Barnes, A. Wander, R. M. Ormerod, D. A. King, and R. M. Lamerod, *Surf. Sci.* **1**, 314 (1994).
- ¹⁷C. J. Baddeley, R. M. Ormerod, A. W. Stephenson, and R. M. Lambert, *J. Phys. Chem.* **99**, 5146 (1996).
- ¹⁸J. P. Perdew and Y. Wang, *Phys. Rev. B* **45**, 13244 (1992).
- ¹⁹D. Vanderbilt, *Phys. Rev. B* **41**, 7892 (1990).
- ²⁰G. Kresse and J. Furthmuller, *Phys. Rev. B* **54**, 11169 (1996).
- ²¹H. J. Monkhorst and J. D. Pack, *Phys. Rev. B* **13**, 5188 (1976).
- ²²As known, this is suitable under the condition that the removed surface Au atoms re-bind with each other somewhere on the surface, e.g., around kink sites.
- ²³H. E. Hoster, E. Filonenko, B. Richter, and R. J. Behm, *Phys. Rev. B* **73**, 165413 (2006).
- ²⁴S. Takizawa, K. Terakura, and T. Mohri, *Phys. Rev. B* **39**, 5792 (1989).
- ²⁵S. E. Mason, I. Ginberg, and A. M. Rappe, *Phys. Rev. B* **69**, 161401(R) (2004).
- ²⁶B. Hammer, L. B. Hansen, and J. K. Nørskov, *Phys. Rev. B* **59**, 7413 (1999).
- ²⁷S. E. Mason, I. Ginberg, and A. M. Rappe, *Phys. Rev. B* **69**, 161401 (2004).
- ²⁸G. Kresse, A. Gil, and P. Sautet, *Phys. Rev. B* **68**, 073401 (2003).
- ²⁹H. Conrad *et al.*, *Surf. Sci.* **43**, 462 (1974).